Life-cycle cost assessment of inelastic buildings with tuned mass dampers in seismic areas

Life-cycle cost assessment of inelastic buildings with tuned mass dampers in seismic areas

Emiliano Matta

Department of Structural, Geotechnical and Building Engineering,
Politecnico di Torino,
C.so Duca degli Abruzzi 24, 10129 Turin, Italy
E-mail: emiliano.matta@polito.it

Abstract: A methodology is presented for evaluating, in a life-cycle cost (LCC) perspective, the seismic effectiveness of passive tuned mass dampers (TMDs) on inelastic building structures. Traditional assessment criteria reveal that TMD performance largely depends on the extent of response non-linearity and therefore on the seismic intensity level, proving satisfactory under moderate earthquakes but negligible under strong ones. Yet those criteria cannot provide a concise measure of control advantages, since they cannot weigh, on a physically sound, economic basis, the relative impact of different hazard levels. Through estimating the occurrence probability and expected lifetime cost of future seismic damages and losses, a multi-hazard LCC approach is here proposed as an efficient alternative for TMD cost-effectiveness assessment. An illustrative example shows that retrofitting a TMD on typical low-rise steel office structures in high seismicity regions may significantly reduce the building lifetime cost despite the detrimental effect observed under collapse limit state.

Keywords: cost effectiveness; life-cycle cost; LCC; seismic risk; tuned mass dampers; TMD; inelastic structures; performance-based engineering; existing buildings.

Reference to this paper should be made as follows: Matta, E. (xxxx) 'Life-cycle cost assessment of inelastic buildings with tuned mass dampers in seismic areas', *Int. J. Lifecycle Performance Engineering*, Vol. X, No. Y, pp.xxx–xxx.

Biographical notes: Emiliano Matta is a Post-doc Research Fellow at the Department of Structural, Geotechnical and Building Engineering at Politecnico di Torino (Turin, Italy), where he received his Master in Civil Engineering in 2002 and his PhD in Structural Engineering in 2006. He is the author of numerous papers on top rank international journals, mostly in the fields of structural dynamics and seismic engineering, vibration control and structural health monitoring. He has a long-term experience as a Professional and Consultant Engineer, mainly on the themes of structural design, seismic and forensic engineering.

1 Introduction

Widely used to control the dynamic response of flexible civil structures subjected to quasi-stationary dynamic loads (winds, sea waves, pedestrians), passive tuned mass

dampers (TMDs) are more rarely employed for the seismic protection of buildings, their effectiveness in earthquake mitigation still being a debated research topic.

Numerous results show that TMDs can satisfactorily reduce the seismic response of structures as long as these remain linear. Their effectiveness proves larger for long-duration narrow-band ground motions but has recently been proven acceptable even against impulsive earthquakes provided that sufficiently large mass ratios and proper design techniques are adopted (Hoang et al., 2008; Matta, 2011).

More controversial appears their effectiveness on inelastic structures. Investigating the performance of TMDs on single- and multi-storey inelastic structures under historical seismic records, several studies conducted in the '80s and '90s (Kaynia et al., 1981; Sladek and Klingner, 1983; Soto-Brito and Ruiz, 1999) reveal a substantial TMD control degradation with increasing earthquake intensity; as the main structure deeply enters into the non-linear range as a result of high-intensity ground motions, insignificant reductions in the peak values of displacement and acceleration time-histories are observed. Considering the peak response reduction as an insufficient criterion, more recent contributions (Lukkunaprasit and Wanitkorkul, 2001; Pinkaew et al., 2003) adopt the accumulated hysteretic energy ratio as the performance index to measure the low-cycle fatigue damage induced by ground motion; these studies suggest that, although a TMD cannot effectively reduce the peak displacement after yielding, it can significantly reduce fatigue damage under moderate earthquakes. The same energy perspective is adopted by Wong (2008), proving that TMDs enhance the ability of inelastic structures to withstand strong earthquakes by storing large amounts of energy at the critical moments and subsequently releasing them in the form of damping energy. An approach based on seismic fragility curves is adopted by Wong and Harris (2012), confirming the capability of TMDs to dissipate energy at low levels of earthquake shaking but at the same time their performance reduction under strong earthquakes. The effectiveness of TMDs on weakly-non-linear structures in areas subjected to narrow-band long-distance earthquakes is explored by Zhang and Balendra (2013); through applying a proper optimisation criterion to a TMD having 2% mass ratio, a 19% displacement reduction can be obtained instead of the 16% achieved with traditional design methods.

As a result, current literature tends to generally recognise TMDs as effective under moderate earthquake loading, when the structure remains linear or weakly non-linear, whilst prone to failure under severe ground shaking, when the structural response becomes strongly non-linear. However, traditional performance criteria, no matter if based on peak response or energy reduction evaluation, appear inadequate to provide a concise measure of control advantages, since they cannot weigh, on a physically sound, economic basis, the relative significance of different hazard levels. A fair and comprehensive assessment of TMDs seismic efficiency should rather be based on determining, through a probabilistic seismic hazard analysis, to which extent moderate and severe earthquakes respectively contribute to the expected damage cost over the lifespan of the structure, which can ultimately be accomplished by establishing how TMDs impact on the structure life-cycle cost (LCC).

LCC assessment is a decision-support tool increasingly used in earthquake engineering as a structural performance criterion accounting for the expected cost of future seismic damages and losses, defined by applying a cost factor to the failure probability of the structure. By applying the LCC concept, instead of merely looking at an asset in terms of costs to design and build (initial cost), investors and managers can broaden their perspective including all operation, maintenance, repair, replacement and

disposal costs over a period of time (lifetime cost). The sum of the initial and the lifetime costs determines the total LCC of the building, whose minimisation should be regarded as the primary objective of any optimal design procedure, either in the construction of new assets or in the improvement of existing ones. LCC assessment of structures in seismic areas has been the subject of several papers in the last decade (e.g., Kappos and Dimitrakopoulos, 2008), including some recent works devoted to passive (Taflanidis and Beck, 2009) and semi-active (Hahm et al., 2013) control strategies, but none of these has dealt so far with TMDs seismic assessment, to the best of the author's knowledge.

In the present paper, a method for evaluating, in a LCC perspective, the seismic effectiveness of TMDs on inelastic building structures is described and applied to a simulated case study consisting in the seismic retrofit of a passive TMD on the SAC Steel Project three-storey benchmark building (Gupta and Krawinkler, 1999), the latter being chosen as representative of typical low-size steel moment-resisting frame (MRF) office buildings designed for high seismic hazard regions.

2 Methodology

Among the several methods recently developed for estimating building lifetime cost in earthquake engineering (Taflanidis and Beck, 2009), the approach developed by Wen and Kang (2001) and subsequently improved by Lagaros and co-authors (e.g., Lagaros et al., 2006; Fragiadakis and Lagaros, 2011; Mitropoulou et al., 2011) is particularly appealing for its simplicity. It makes damage and consequently lifetime cost depend, for the assigned structural type (e.g., steel MRF buildings), exclusively on seismic demand, expressed by the peak inter-storey drift ratio and evaluated at multiple hazard levels through static or dynamic non-linear analyses. Since TMD-structure interaction can only be quantified by working in the time domain, the approach based on non-linear dynamic analyses is herein implemented.

2.1 Damage index evaluation

In earthquake engineering, LCC assessment demands the calculation of the cost components that are related to the performance of the structure in multiple seismic hazard levels. In the present study, the so-called multiple-stripe dynamic analysis (MSDA) is adopted, one of the most applied multiple-hazard methods implementing non-linear dynamic analysis. In MSDA, many groups of non-linear dynamic analyses (stripes) are performed at increasing intensity levels, each level corresponding to a predetermined exceedance probability in a given time period. The suite of ground motion records used for performing each stripe analysis should be representative of the seismic threat at the corresponding intensity level, according to the hazard curve of the area of interest. The main objective of MSDA is to express the relation existing between the seismic intensity level, described by a parameter (or a vector of parameters) known as the intensity measure (IM), and the corresponding structural response, described by an engineering demand parameter known as the damage index (DI). A probabilistic seismic hazard analysis is usually performed to characterise IMs for different hazard levels, taking into account all important sources of modelling uncertainty for the ground motions. Then, for each of these levels, ground motion records consistent with the corresponding IMs are

selected from some strong-motion database by performing a seismic hazard disaggregation. These recorded ground motions are used in structural analyses to give samples of the structural response, finally providing the DI needed in cost estimation. Due to the complexity and the computational effort required by 3D structural models, simplified 2D simulations are frequently used.

Selecting IM and DI represents two fundamental steps in MSDA. The IM is typically a monotonically scalable ground motion intensity measure like, among others, the peak ground acceleration, the peak ground velocity or the 5% damped spectral acceleration at the structure's first-mode period. On the other hand, a number of DIs are available for seismic damage evaluation (Ghobarah et al., 1999). There is wide consensus that for MRF buildings the storey drift demand, expressed by the inter-storey drift ratio θ, is the best representative among DIs based on maximum deformation (Gupta and Krawinkler, 1999). An established relation exists between θ and performance-oriented descriptions, such as immediate occupancy, life safety and collapse prevention (FEMA-273, 1997). Definite relations, required for LCC assessment, are also available between θ and damage state, for both reinforced concrete buildings (Ghobarah, 2004) and steel frame structures (Wen and Kang, 2001).

In order to perform MSDA, seven hazard levels will be considered in this paper, each described by a set of ten two-components earthquake records selected to be compatible with the earthquake response spectrum expected at the site. The peak inter-storey drift ratio θ will be used as the DI and the relation between damage state and inter-storey drift ratio will be assumed as the one proposed by Wen and Kang (2001) for steel MRF structures, reproduced in Table 1. More exactly, the 2D FE structural model will be separately evaluated under each component of any record so as to obtain the component-DI; then the larger of the two component-DIs of each record will be taken as the record-DI; and finally the mean among all record-DIs of each set of records will give the set-DI, eventually used for cost assessment.

Table 1 Damage states in terms of drift ratio

Damage state		*Drift ratio θ (%)*
1	None	$0.0 \le \theta < 0.2$
2	Slight	$0.2 \le \theta < 0.5$
3	Light	$0.5 \le \theta < 0.7$
4	Moderate	$0.7 \le \theta < 1.5$
5	Heavy	$1.5 \le \theta < 2.5$
6	Major	$2.5 \le \theta < 5.0$
7	Destroyed	$5.0 \le \theta$

Source: Wen and Kang (2001)

2.2 Cost evaluation

The expected total cost C_{TOT} of a structure, over a time period t which may be the design life of a new structure or the remaining life of a retrofitted structure, can be expressed as a function of t as follows (Wen and Kang, 2001, Lagaros et al., 2006):

$$C_{TOT}(t) = C_{IN} + C_{DS}(t) \tag{1}$$

where C_{IN} is the initial cost of a new or retrofitted structure and C_{DS} is the additional cost over the lifetime of the structure, defined as the present value of future damage states cost. C_{IN} comprises the material and labour costs required for the construction of a new building or the retrofitting of an existing one, including structural and non-structural components. Focusing in this study on seismic risk, i.e., neglecting damages caused by other hazards or related to structural and material degradation, C_{DS} expresses the potential damage cost from earthquakes that may occur during the life of the structure, i.e., the seismic lifetime cost. It accounts for the cost of structural and non-structural repair, the cost of loss of contents, the cost of injury recovery or human fatality and other direct or indirect economic losses (e.g., rental and income costs), after an earthquake.

Table 2 Damage state cost calculation formulas

Cost category	*Calculation formula*	*Basic cost*
Damage repair	Replacement cost × floor area × mean damage index	1,500 €/m^2
Loss of content	Unit content cost × floor area × mean damage index	500 €/m^2
Rental	Rental rate × gross leasable area[b] × disruption period[c] × loss of function index	10 €/month/m^2
Income	Income rate × gross leasable area[b] × disruption period[c] × down time index	2,000 €/year/m^2
Minor injury	Minor injury cost per person × floor area × occupancy rate[a] × expected minor injury rate	2,000 €/person
Serious injury	Serious injury cost per person × floor area × occupancy rate[a] × expected serious injury rate	$2 \cdot 10^4$ €/person
Human fatality	Death cost per person × floor area x occupancy rate[a] × expected death rate	$2.8 \cdot 10^6$ €/person

Notes: [a]Occupancy rate: 2 persons/100 m^2
[b]Gross leasable area: 90% of the total floor area
[c]Disruption period: six months

Source: Wen and Kang (2001)

Considering N possible damage states (N = 7 in the present case study, see again Table 1), the damage cost for the i^{th} damage state can be formulated as follows (Mitropoulou et al., 2011):

$$C_{DS}^{i} = C_{dam}^{i} + C_{con}^{i} + C_{ren}^{i} + C_{inc}^{i} + C_{inj}^{i} + C_{fat}^{i} \tag{2}$$

where C_{dam}^{i} is the damage repair cost, C_{con}^{i} is the loss of contents cost, C_{ren}^{i} is the loss of rental cost, C_{inc}^{i} is the income loss cost, C_{inj}^{i} is the injury cost and C_{fat}^{i} is the human fatality cost. The detailed formulas for computing each damage state cost are provided in

Table 2, where the basic costs reported in the third column represent (expressed in euros) the first component of the calculation formulas given in the second column. The values of the damage state parameters are reported in Table 3 and derived by Mitropoulou et al. (2011).

Table 3 Damage state parameters for cost evaluation

Damage state		*Mean damage index (%)*	*Loss of function index (%)*	*Down time index (%)*	*Expected minor injury rate*	*Expected serious injury rate*	*Expected death rate*
1	None	0	0	0	0	0	0
2	Slight	0.5	0.9	0.9	$3.0 \cdot 10^{-5}$	$4.0 \cdot 10^{-6}$	$1.0 \cdot 10^{-6}$
3	Light	5	3.33	3.33	$3.0 \cdot 10^{-4}$	$4.0 \cdot 10^{-5}$	$1.0 \cdot 10^{-5}$
4	Moderate	20	12.4	12.4	$3.0 \cdot 10^{-3}$	$4.0 \cdot 10^{-4}$	$1.0 \cdot 10^{-4}$
5	Heavy	45	34.8	34.8	$3.0 \cdot 10^{-2}$	$4.0 \cdot 10^{-3}$	$1.0 \cdot 10^{-3}$
6	Major	80	65.4	65.4	$3.0 \cdot 10^{-1}$	$4.0 \cdot 10^{-2}$	$1.0 \cdot 10^{-2}$
7	Destroyed	100	100	100	$4.0 \cdot 10^{-1}$	$4.0 \cdot 10^{-1}$	$2.0 \cdot 10^{-1}$

Source: Mitropoulou et al. (2011)

Based on a Poisson process model of earthquake occurrences and an assumption that damaged buildings are fully and quickly restored to their original intact conditions after each significant seismic attack, the damage state cost in equation (1) can be computed (Wen and Kang, 2001) as:

$$C_{DS}(t) = \nu\left(\frac{1-e^{-\lambda t}}{\lambda}\right)\sum_{i=1}^{N} C_{DS}^{i} P_{o}^{i} \tag{3}$$

where P_o^i is the probability of occurrence of the i^{th} damage state given the occurrence of a significant earthquake; ν is the mean frequency of occurrence of significant earthquakes, modelled by a Poisson process; and λ is the momentary discount rate, which actualises future costs to their current value (typically taken as 3%–5%/year). The ratio in parenthesis, which tends to t for λ tending to 0, represents the actualised time period t_a, so that equation (3) can be more clearly rewritten as:

$$C_{DS}(t) = t_a \sum_{i=1}^{N} C_{DS}^{i} \phi_b^i \tag{4}$$

where $\phi_b^i = \nu P_o^i$ represents the mean frequency of occurrence of the i^{th} damage state. Following Wen and Kang (2001), the i^{th} damage state is identified by the drift ratio limits listed in Table 1. When one of those limits is exceeded, the corresponding damage state is reached. The mean frequency of occurrence ϕ_b^i of the i^{th} state in equation (4) can be therefore expressed by:

$$\phi_b^i = \phi_e^i - \phi_e^{i+1} \tag{5}$$

where ϕ_e^i is the mean frequency of exceedance of θ_i and can be computed using a relation of the form:

$$\phi_e^i = f(\theta_i) \tag{6}$$

Such relation is deduced by fitting a properly shaped function f to a number M of known $\phi_e^j - \theta_j$ pairs, corresponding to the sets of earthquake records defined at M preselected, increasing hazard levels, where the j^{th} hazard level is characterised by a known probability of exceedance $P_{e/\tau}^j$ in a given period of time τ. For each pair, i.e., for each hazard level, the drift ratio θ_j is taken as the set-DI computed by non-linear dynamic analyses, while the mean frequency of exceedance of θ_j is derived, according to Poisson's law, as:

$$\phi_e^j = -\frac{1}{\tau}\ln\left(1 - P_{e/\tau}^j\right) \tag{7}$$

In previous works by, e.g., Lagaros et al. (2006) and Mitropoulou et al. (2011), the function f in equation (6) was obtained by a least-square fitting of the M pairs through an expression of the form:

$$f(\theta) = \alpha\theta^{-\beta} \tag{8}$$

Depending on two fitting parameters, α and β, this hyperbolic expression ensures an exact fitting only for $M = 2$, while for $M > 2$ it generally entails some error. In the present application, the error was observed to become unacceptably large already for M as small as 3 or 4, resulting in biased cost estimates, and equation (8) was thus concluded to be unable to accurately reproduce the relationship in equation (6). Also, taking $M = 3$, as in some previous studies, proved here insufficient to sample the entire domain of possible $\phi_e^j - \theta_j$ pairs. Various alternative forms of f were then explored, which could satisfactorily fit equation (6) for larger values of M (for instance $M = 7$ as in the illustrative example presented in the next section). A good compromise between simplicity and accuracy was obtained adopting the following function:

$$f(\theta) = \begin{cases} \alpha_1\theta^{-\beta_1} & \text{for } \theta < \theta_2 \\ \gamma\left(\alpha_j\theta^{-\beta_j}\right) + (1-\gamma)\left(a_j\theta + b_j\right) & \text{for } \theta_j \le \theta < \theta_{j+1},\ j = 2,\ldots,M-2 \\ \alpha_{M-1}\theta^{-\beta_{M-1}} & \text{for } \theta \ge \theta_{M\text{-}1} \end{cases} \tag{9}$$

where α_j and β_j are analytically determined so that the hyperbolic expression $\alpha_j\theta^{-\beta_j}$ exactly interpolates pairs j and j+1, a_j and b_j are analytically determined so that the linear expression $a_j\theta + b_j$ exactly interpolates pairs j and j+1, and γ is numerically determined so that the sum of the changes of slope of $f(\theta)$ at every θ_j, expressed by $\sum_{j=2}^{M-1}\left|f'_+(\theta_j) - f'_-(\theta_j)\right|$, shall be minimum. In the range $[\theta_2, \theta_{M\text{-}1}]$, equation (9) provides the weighed sum of the hyperbolic interpolation and the linear interpolation of the $M - 2$ internal pairs, performed independently between any two consecutive pairs. Outside that range, equation (9) provides the hyperbolic interpolation (and extrapolation) of the two outermost couples (respectively left and right) of $\phi_e^j - \theta_j$ pairs. Thus, equation (9) ensures a function passing through all the available M pairs. The numerical minimisation

required to identify the optimal weight γ can be easily performed through any available technique, including a simple trial and errors search. A graphical representation of equation (9) is exemplified in Figure 6 and will be discussed in greater detail later.

Unlike in previous works (e.g., Wen and Kang, 2001; Lagaros et al., 2006), where the drift ratio was taken as the maximum over the entire building height, in the present study the damage and costs at any given storey are assumed to depend on the drift ratio measured at that storey; the global building cost then follows as the mere summation of all the storey-level costs. The only exception is represented by costs related to the collapse damage state ('7 – destroyed'), which are assumed to be governed, for all storey levels, by the largest drift ratio along the building height, as if the collapse of any one storey implied the collapse of the entire building. Operatively, this requires that the frequency of occurrence at the collapse damage state ('7 – destroyed'), ϕ_b^7, be increased, for every single storey, from its respective value to the value corresponding to the global DI defined as the maximum drift along the building height. At the same time, for each storey, the amount added to ϕ_b^7 shall be removed from ϕ_b^6, representing the frequency of occurrence of the previous damage state ('6 – major'). With respect to previous studies, the slight increase in complexity of this variant is largely repaid by the improved accuracy of the cost estimation, especially in the case when most damage is localised at few storey levels.

It deserves noticing that, according to the exposed methodology, the building lifetime cost, C_{DS}, exclusively represents the expected cost of future seismic damages and does not include other costs, such as costs of damages caused by other hazards or related to structural or material degradation. In such an LCC analysis, the consequences of an earthquake striking at any time in the future are evaluated assuming that the structure shall react as if newly constructed, i.e., as if any structural damage or degradation possibly occurred prior to that seismic event had been fully and promptly recovered in the meanwhile. This condition certainly entails periodical reassessment and monitoring activities aimed at ensuring at all times that the structural performance of the building shall be as good as expected at the beginning of its life. Such activities are therefore a necessary prerequisite to apply the proposed LCC assessment methodology in its present form. The cost related to such activities does not enter into the building lifetime cost as defined above and, most relevantly for the present study, proves essentially independent on the building being or not retrofitted with a TMD, so that neglecting such term in finally balancing the two latter options does not substantially affect the evaluation of TMD seismic performance.

It also deserves mentioning that no damage of the TMD is considered in the present study. As it should be in real-case applications, the newly installed TMD is assumed to be properly designed and periodically monitored so as to safely and effectively respond to any of the seismic intensities expected at the site during the whole building lifetime. Moreover, no explicit account of possible mistuning effects is given here as well. Previous studies (Hoang et al., 2008; Matta, 2011) indicate that TMD performance loss due to mistuning is nearly negligible if sufficiently high mass ratios are used. The same monitoring action will also allow periodical recalibration of the device's frequency, further limiting mistuning consequences.

3 Example

The seismic effectiveness of installing a TMD on an existing standard low-rise office building is assessed by comparing the building lifetime cost, evaluated as explained in the previous Section, respectively in the absence and in the presence of the TMD atop. The chosen building is a standard perimeter steel MRF structure located in Los Angeles (California). Because of the in-plan symmetric arrangement of the moment-resisting frames, structural analysis and cost evaluation will be performed using a planar (2D) model of the building along the N-S direction only.

3.1 The structural model

3.1.1 The uncontrolled model

The case study is the three-storey steel MRF building designed for Los Angeles by Brandow & Johnston Associates within the SAC Phase II Steel Project (Gupta and Krawinkler, 1999), and later turned into one of the three benchmark control problems for seismically excited non-linear buildings described in Ohtori et al. (2004). The structure was designed as a standard low-rise office building on stiff soil (soil type S2) according to UBC 1994, following all code requirements for gravity, wind and seismic design. Although not actually constructed, the building can be considered representative of typical steel MRFs in LA, designed according to pre-Northridge design practice.

The benchmark structure is 36.58 m by 54.87 m in plan and 11.89 m in elevation. The bays are 9.15 m in both directions, with four bays in the North-South (N-S) direction and six bays in the East-West (E-W) direction. The lateral load-resisting system is made of perimeter steel MRFs with simple framing between the two furthest South E-W frames. The interior bays of the structure contain simple framing with composite floors. The building comprises one ground level and three above-ground storey levels, the third of which is the roof. Floor-to-floor height is 3.96 m. The column bases are modelled as fixed to the ground. Dimensions and materials of columns and beams are detailed in Gupta and Krawinkler (1999). The inertial effects of each level are assumed to be carried evenly by the floor diaphragm to each perimeter MRF, hence each frame resists one half of the seismic mass of the entire structure .The seismic mass of the first and second levels is $9.57 \cdot 10^5$ kg, that of the third level is $1.04 \cdot 10^6$ kg. The N-S MRF is sketched in Figure 1.

Figure 1 Schematics of the three-storey building, (a) elevation (b) plan

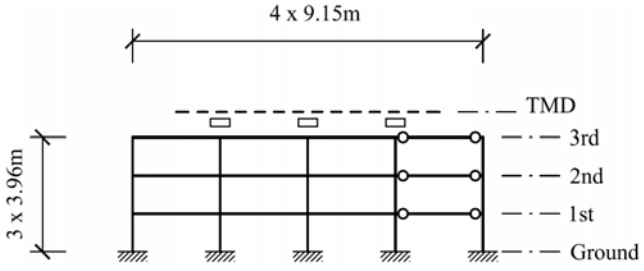

(a)

Figure 1 Schematics of the three-storey building, (a) elevation (b) plan (continued)

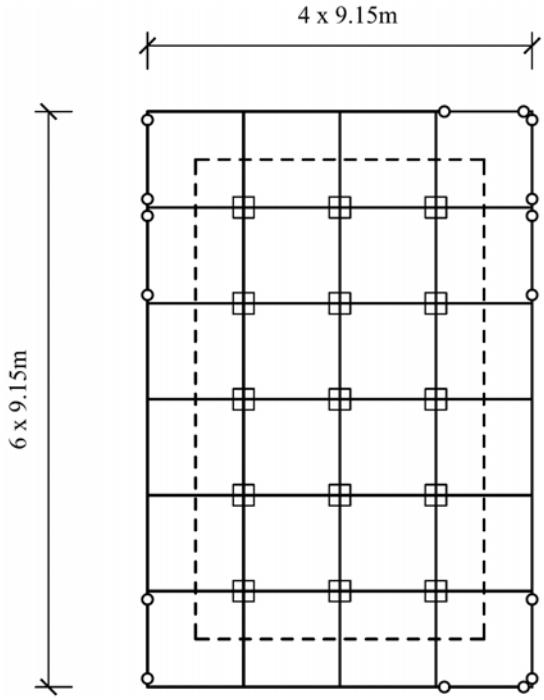

(b)

The uncontrolled structural model is the 2D non-linear FE representation of the two N-S MRFs of the benchmark building. The model is as the one implemented by Ohtori et al. (2004) in a set of MATLAB files made available on the web (*http://www.nd.edu/~quake/*), except that in the present version it has been modified so as to account for second order (P-delta) effects and to allow incorporation of a TMD into the model.

The model represents a ductile steel MRF structure with no strength and stiffness degradation in the element characteristics and no connection weld fractures. A concentrated plasticity model is assumed, with members remaining elastic and yielding occurring only at their ends, where point plastic hinges are described by a bilinear moment-rotation relationship with 3% strain-hardening. The damping matrix is determined based on an assumption of Rayleigh damping, enforcing a 2% damping ratio onto the first two modes.

As long as the structure responds in the linear elastic range, the first three natural frequencies of the uncontrolled structure are 0.990 Hz, 3.056 Hz and 5.827 Hz for the model evaluated excluding second order effects, and 0.977 Hz, 3.031 Hz and 5.792 Hz for the model evaluated including second order effects.

3.1.2 The controlled model

The controlled structural model is obtained by attaching to the top storey of the uncontrolled structural model a linear SDOF model of a TMD, characterised by a mass m_t, a circular frequency ω_t and a damping ratio ζ_t. The mass m_t is fixed by the designer as a given percentage of the total structural mass m_s through assigning the mass ratio $\mu = m_t/m_s$, whereas ω_t and ζ_t are chosen so as to achieve the optimum tuning of the absorber to the fundamental mode of the building. More precisely, denoting by ω_s and ζ_s respectively the circular frequency and the damping ratio of the target mode, by $m_{s,eff}$ its effective modal mass, defined (Warburton, 1982) as the target modal mass divided by the squared amplitude of the mass-normalised target mode shape at the TMD position, and finally denoting by $\mu_{eff} = m_t/m_{s,eff}$ and $r = \omega_t/\omega_s$ respectively the effective mass ratio and the frequency ratio of the TMD, then the typical design procedure consists in:

1 arbitrarily fixing μ_{eff}

2 accordingly finding r and ζ_t which make the control optimal with respect to some desired objective.

Figure 2 Uncontrolled and controlled transfer functions from the ground acceleration to the maximum inter-storey drift ratio

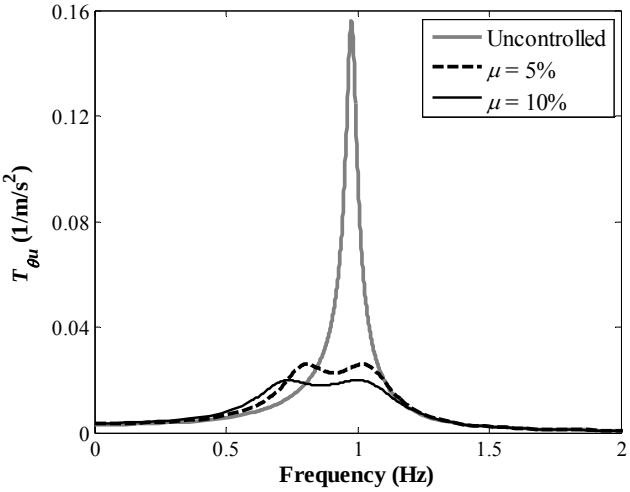

Table 4 Design control parameters for two possible values of the TMD mass ratio

Mass ratio μ	*Effective mass ratio* μ_{eff}	*Circular frequency* ω_s	*Frequency ratio* r	*Damping ratio* ζ_t
5%	9.69%	6.132 rad/s	88.1%	17.6%
10%	19.4%	6.125 rad/s	80.3%	24.3%

In most applications, optimality is identified with the minimisation of the H_2-norm (Hoang et al., 2008) or the H_∞-norm (Sladek and Klingner, 1983; Pinkaew et al., 2003; Matta et al., 2009) of some input-output transfer functions (TF) of the controlled system. In the present study, the TF from the ground acceleration to the maximum inter-storey drift ratio, denoted as $T_{\theta u}$, is adopted, and the H_∞^f approach proposed in Matta (2011) is applied, which consists in the numerical minimisation of the H_∞-norm of $T_{\theta u}$ multiplied by a Kanai-Tajimi filter whose circular frequency ω_g equals the structural frequency ω_s and whose damping ratio ζ_g is set to 0.3. The linearised structural model used for computing $T_{\theta u}$ is the one accounting for II order effects. Two alternative mass ratios are considered, namely μ = 5% and μ = 10%. For each mass ratio, the optimum frequency and damping ratios, r and ζ_t, are numerically found which minimise the filtered $T_{\theta u}$. Results are summarised in Table 4. Thus, for example, if the 10% mass ratio is chosen, the optimal TMD will be a SDOF appendage having mass $m_t = 2.949 \cdot 10^5$ kg, circular frequency ω_t = 4.920 rad/s and damping ratio ζ_t = 24.3%, or alternatively stiffness k_t = 7.137 kN/mm and damping coefficient c_t = 0.705 kNs/mm. Uncontrolled and controlled transfer functions $T_{\theta u}$ are shown in Figure 2 for comparison.

3.2 The seismic loading

M = 7 hazard levels are considered in this present case study, whose probabilities of exceedance $P_{e/\tau}^j$ in the period τ and mean frequencies of exceedance ϕ_e^j are summarised in Table 5. Each hazard level is described by a set of 20 time histories: ten ground motions each with two orthogonal components. All sets are defined in accordance to the seismic hazard at the building site. Sets 5 to 7 (details of the ground motions in each set are reported in Tables 6 to 8) are taken from the SAC steel research project (Somerville et al., 1997), consisting of recorded and simulated ground motions representing probabilities of exceedance equal to, respectively, 50% in 50 years, 10% in 50 years and 2% in 50 years. All ground motions are rotated to 45° with respect to the fault in order to minimise directivity effects and are scaled such that, on average, their spectral ordinates would match with a least square error fit the US Geological Survey's (USGS) mapped spectral values at 0.3, 1.0 and 2.0 seconds, and an additional predicted value at 4.0 seconds. The weights assigned to the four period points are 0.1 for 0.3 s and 0.3 for the other three period points (Gupta and Krawinkler, 1999). On the other hand, sets 1 to 4 are obtained through simply scaling all records in set 5 so that the compatibility with the USGS spectral values is still ensured on average at the same four period points. In Figure 3, the individual (grey lines) and mean (black line) 5% damped elastic pseudo-acceleration spectra are plotted for sets 5 to 7.

Table 5 The M = 7 multiple hazard levels considered in the present study

Set # j	*1*	*2*	*3*	*4*	*5*	*6*	*7*
$P_{e/\tau}^j$ (%)	50	50	50	50	50	10	2
τ (years)	2	5	10	30	50	50	50
ϕ_e^j (n/year)	$3.466 \cdot 10^{-1}$	$1.386 \cdot 10^{-1}$	$6.931 \cdot 10^{-2}$	$2.310 \cdot 10^{-2}$	$1.386 \cdot 10^{-2}$	$2.107 \cdot 10^{-3}$	$4.041 \cdot 10^{-4}$

Table 6 Ground motion records in set 5%–50% probability of exceedance in 50 years

Designation	*Record*	M_W	*Distance (km)*	*Scale factor*	*Duration (s)*	*PGA (cm/s^2)*
LA41	Coyote Lake, 1979	5.7	8.8	2.28	39.38	578.34
LA42	Coyote Lake, 1979	5.7	8.8	2.28	39.38	326.81
LA43	Imperial Valley, 1979	6.5	1.2	0.4	39.08	140.67
LA44	Imperial Valley, 1979	6.5	1.2	0.4	39.08	109.45
LA45	Kern, 1952	7.7	107	2.92	78.6	141.49
LA46	Kern, 1952	7.7	107	2.92	78.6	156.02
LA47	Landers, 1992	7.3	64	2.63	79.98	331.22
LA48	Landers, 1992	7.3	64	2.63	79.98	301.74
LA49	Morgan Hill, 1984	6.2	15	2.35	59.98	312.41
LA50	Morgan Hill, 1984	6.2	15	2.35	59.98	535.88
LA51	Parkfield, 1966, Cholame 5W	6.1	3.7	1.81	43.92	765.65
LA52	Parkfield, 1966, Cholame 5W	6.1	3.7	1.81	43.92	619.36
LA53	Parkfield, 1966, Cholame 8W	6.1	8	2.92	26.14	680.01
LA54	Parkfield, 1966, Cholame 8W	6.1	8	2.92	26.14	775.05
LA55	North Palm Springs, 1986	6	9.6	2.75	59.98	507.58
LA56	North Palm Springs, 1986	6	9.6	2.75	59.98	371.66
LA57	San Fernando, 1971	6.5	1	1.3	79.46	248.14
LA58	San Fernando, 1971	6.5	1	1.3	79.46	226.54
LA59	Whittier, 1987	6	17	3.62	39.98	753.70
LA60	Whittier, 1987	6	17	3.62	39.98	469.07

Source: Somerville et al. (1997)

Table 7 Ground motion records in set 6%–10% probability of exceedance in 50 years

Designation	*Record*	M_W	*Distance (km)*	*Scale factor*	*Duration (s)*	*PGA (cm/s^2)*
LA01	Imperial Valley, 1940, El Centro	6.9	10	2.01	39.38	452.03
LA02	Imperial Valley, 1940, El Centro	6.9	10	2.01	39.38	662.88
LA03	Imperial Valley, 1979, Array #05	6.5	4.1	1.01	39.38	386.04
LA04	Imperial Valley, 1979, Array #05	6.5	4.1	1.01	39.38	478.65
LA05	Imperial Valley, 1979, Array #06	6.5	1.2	0.84	39.08	295.69
LA06	Imperial Valley, 1979, Array #06	6.5	1.2	0.84	39.08	230.08
LA07	Landers, 1992, Barstow	7.3	36	3.2	79.98	412.98
LA08	Landers, 1992, Barstow	7.3	36	3.2	79.98	417.49
LA09	Landers, 1992, Yermo	7.3	25	2.17	79.98	509.70
LA10	Landers, 1992, Yermo	7.3	25	2.17	79.98	353.35
LA11	Loma Prieta, 1989, Gilroy	7	12	1.79	39.98	652.49
LA12	Loma Prieta, 1989, Gilroy	7	12	1.79	39.98	950.93

Source: Somerville et al. (1997)

Table 7 Ground motion records in set 6%–10% probability of exceedance in 50 years (continued)

Designation	*Record*	M_W	*Distance (km)*	*Scale factor*	*Duration (s)*	*PGA (cm/s^2)*
LA13	Northridge, 1994, Newhall	6.7	6.7	1.03	59.98	664.93
LA14	Northridge, 1994, Newhall	6.7	6.7	1.03	59.98	644.49
LA15	Northridge, 1994, Rinaldi RS	6.7	7.5	0.79	14.945	523.30
LA16	Northridge, 1994, Rinaldi RS	6.7	7.5	0.79	14.945	568.58
LA17	Northridge, 1994, Sylmar	6.7	6.4	0.99	59.98	558.43
LA18	Northridge, 1994, Sylmar	6.7	6.4	0.99	59.98	801.44
LA19	North Palm Springs, 1986	6	6.7	2.97	59.98	999.43
LA20	North Palm Springs, 1986	6	6.7	2.97	59.98	967.61

Source: Somerville et al. (1997)

Table 8 Ground motion records in set 7%–2% probability of exceedance in 50 years

Designation	*Record*	M_W	*Distance (km)*	*Scale factor*	*Duration (s)*	*PGA (cm/s^2)*
LA21	1995 Kobe	6.9	3.4	1.15	59.98	1258.0
LA22	1995 Kobe	6.9	3.4	1.15	59.98	902.75
LA23	1989 Loma Prieta	7	3.5	0.82	24.99	409.95
LA24	1989 Loma Prieta	7	3.5	0.82	24.99	463.76
LA25	1994 Northridge	6.7	7.5	1.29	14.945	851.62
LA26	1994 Northridge	6.7	7.5	1.29	14.945	925.29
LA27	1994 Northridge	6.7	6.4	1.61	59.98	908.70
LA28	1994 Northridge	6.7	6.4	1.61	59.98	1304.1
LA29	1974 Tabas	7.4	1.2	1.08	49.98	793.45
LA30	1974 Tabas	7.4	1.2	1.08	49.98	972.58
LA31	Elysian Park (simulated)	7.1	17.5	1.43	29.99	1271.2
LA32	Elysian Park (simulated)	7.1	17.5	1.43	29.99	1163.5
LA33	Elysian Park (simulated)	7.1	10.7	0.97	29.99	767.26
LA34	Elysian Park (simulated)	7.1	10.7	0.97	29.99	667.59
LA35	Elysian Park (simulated)	7.1	11.2	1.1	29.99	973.16
LA36	Elysian Park (simulated)	7.1	11.2	1.1	29.99	1079.3
LA37	Palos Verdes (simulated)	7.1	1.5	0.9	59.98	697.84
LA38	Palos Verdes (simulated)	7.1	1.5	0.9	59.98	761.31
LA39	Palos Verdes (simulated)	7.1	1.5	0.88	59.98	490.58
LA40	Palos Verdes (simulated)	7.1	1.5	0.88	59.98	613.28

Source: Somerville et al. (1997)

3.3 Traditional performance criteria for TMD assessment

Nine traditional performance criteria are drawn from the literature in order to evaluate TMD effectiveness under the seven sets of earthquake records. These criteria are dimensionless quantities defined by dividing the controlled mean response computed for each record set by the corresponding uncontrolled mean response (Ohtori et al., 2004). They fall into two main categories: building response and building damage. The first category comprises three peak response measures, namely: the maximum peak inter-storey drift ratio (J_1), the maximum peak acceleration (J_2) and the peak base shear force (J_3), together with their three root mean square (RMS) counterparts, namely: the maximum RMS inter-storey drift ratio (J_4), the maximum RMS acceleration (J_5) and the RMS base shear force (J_6). The term 'peak' is herein used to denote the over-time largest value of any response signal while the term 'maximum' is used to denote the largest value along the building height. The second category comprises three damage measures, namely the number of damaged members' ends (J_7), the maximum dissipated energy factor at members' ends (J_8) and the total dissipated energy factor (J_9). These latter criteria have obviously only meaning for structures undergoing plastic deformations and are, therefore, undefined when the uncontrolled building remains elastic.

Figure 3 Pseudo-acceleration elastic spectra for $\zeta_s = 5\%$

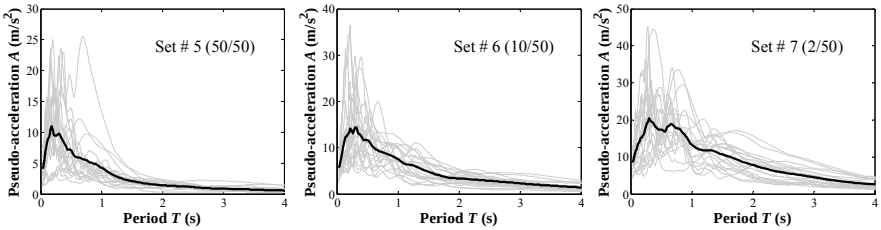

Note: Thin grey lines: individual spectra; thick black lines: mean spectra

Results are reported in Tables 9 and 10, respectively for $\mu = 5\%$ and $\mu = 10\%$. As far as the structure remains linear (sets 1 and 2), a satisfactory TMD performance is observed, which obviously (although not dramatically) proves better for the larger mass ratio, and expectedly proves greater in RMS terms than in peak terms. For example, if $\mu = 10\%$ is chosen, the maximum displacement and the base shear will be reduced to, respectively, 67% and 64% in peak terms, and to 40% and 42% in RMS terms, while the maximum acceleration will notoriously undergo lesser reductions (namely to 79% and 48%, respectively in peak and RMS terms). However, as the structure enters more deeply into its inelastic range under the effect of increasing hazard levels, the TMD performance progressively degrades. The loss of tuning due to structural period shifts makes the TMD increasingly ineffective, and the large inelastic excursions make the building's hysteresis the exceedingly predominant dissipation mechanism. At the highest hazard levels (sets 6 and 7), the control action becomes even detrimental in terms of peak response criteria; the larger the mass ratio, the greater the structural response, with the TMD basically working as an additional inertial mass clamped to the supporting structure. RMS performance undergoes a degradation too, although generally less severe: acceleration (J_5) and base shear (J_6) criteria keep well under unity, while the drift ratio criterion (J_4) increases beyond unity as a consequence of the accumulation of permanent

residual drifts. Also damage-related indices confirm this trend of progressive control reduction; satisfactory results are obtained up to set 5, but under sets 6 and 7 almost all members' ends undergo damage (J_7) and the TMD energy absorption capability (J_8 and J_9) becomes nearly negligible. It can be concluded that, in the considered case study, TMD effectiveness, if measured by traditional performance criteria, dramatically depends on the hazard level, proving of virtually no engineering interest under record sets corresponding to a probability of occurrence equal to or smaller than approximately 10% in 50 years.

Table 9 TMD with μ = 5% – performance indices for the M = 7 hazard levels

Set j	J_1	J_2	J_3	J_4	J_5	J_6	J_7	J_8	J_9
1	0.72	0.85	0.71	0.46	0.53	0.48	-	-	-
2	0.72	0.85	0.71	0.46	0.53	0.48	-	-	-
3	0.72	0.87	0.72	0.46	0.54	0.49	0.64	0.21	0.15
4	0.81	0.92	0.81	0.71	0.62	0.56	0.47	0.21	0.40
5	0.84	0.93	0.89	0.79	0.68	0.61	0.55	0.24	0.39
6	0.98	0.99	1.01	1.01	0.76	0.70	0.97	0.65	0.74
7	1.05	0.98	0.99	1.07	0.86	0.79	0.97	0.89	0.96

Table 10 TMD with μ = 10% – performance indices for the M = 7 hazard levels

Set j	J_1	J_2	J_3	J_4	J_5	J_6	J_7	J_8	J_9
1	0.67	0.79	0.64	0.40	0.48	0.42	-	-	-
2	0.67	0.79	0.64	0.40	0.48	0.42	-	-	-
3	0.68	0.81	0.65	0.40	0.49	0.43	0.18	0.00	0.00
4	0.76	0.88	0.75	0.68	0.58	0.49	0.37	0.17	0.34
5	0.79	0.91	0.86	0.69	0.63	0.54	0.44	0.18	0.33
6	1.00	0.99	1.02	1.02	0.70	0.64	0.94	0.52	0.62
7	1.09	1.01	1.02	1.10	0.82	0.74	0.97	0.82	0.92

3.4 LCC approach for TMD assessment

The procedure presented in Section 2.3 is applied to the three-storey SAC building, with and without a TMD on it. For each storey level, the mean (within each set of records) of the maximum (of the two record components) value of the inter-storey drift ratio provides the θ_j term of each $\phi_k^j - \theta_j$ pair. The function *f(θ)* defined by equation (9) is derived through a numerical minimisation, the optimal weight being found to be γ = 0.8.

The procedure is graphically explained by Figure 4, where the annual frequency of exceedance is expressed as a function of the drift ratio for the second storey level and for the three control cases, i.e., μ = 0% (uncontrolled), μ = 5% and μ = 10%. Similar curves are obtained for the other storeys, as well as for the maximum drift ratio along the building height used for estimating the collapse frequency of occurrence. The black markers represent the 'forward step' of the procedure, which entails performing time-history analyses and averaging among records for each hazard level. The white

markers represent the 'backward step', which implies extracting exceedance and occurrence frequencies for each damage state.

Figure 4 Annual frequency of exceedance as a function of the inter-storey drift ratio, for the 2nd storey level and respectively: μ = 0% (square markers); μ = 5% (circles); μ = 10% (triangles)

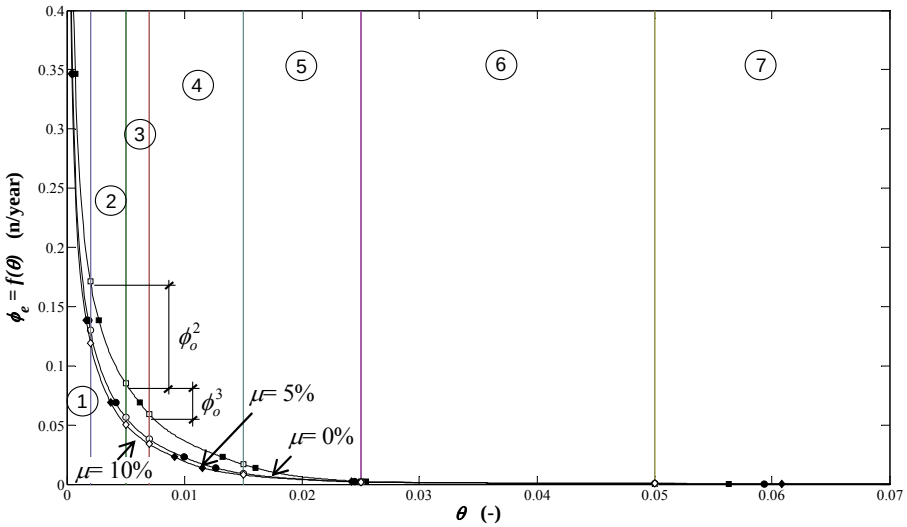

Notes: Black markers: from analyses; white markers: from fitting.

Once the frequency of occurrence is evaluated for all storey levels and for all damage states, the lifetime cost can be computed using equation (4) and Tables 1 to 3, assuming, for the present example, a lifetime period t = 50 years and a momentary discount rate λ = 4%/year.

Results are reported in Figures 5 and 6. In Figure 5, the lifetime cost is decomposed, for the uncontrolled and the two controlled cases, into the seven damage states for each storey level. Since the cost related to the first damage state ('1 – none') is null, only six damage states are visible in the bar graph, from the second one (on the left) to the seventh one (on the right). For the two controlled cases, the white rectangle at the utmost right represents the complement to the uncontrolled cost, included for comparison's sake. The largest part of the damage cost is clearly inflicted within the fourth damage state ('4 – moderate') and secondarily within the fifth one ('5 – heavy'), which achieve the most expensive combination of occurrence probability and damage severity, thus contributing the most to the overall lifetime cost. These intermediate damage states are also those where TMD cost-effectiveness achieves its best. Within the fourth damage state, the TMD reduces lifetime costs to 73% of the uncontrolled value for μ = 5% and to 66% for μ = 10%; within the fifth damage state, the reduction is even larger, to respectively 54% for μ = 5% and 45% for μ = 10%. The third most expensive damage state is the seventh one, corresponding to the collapse limit state ('7 – destroyed'), followed by the sixth one ('6 – major'). Note that costs related to the seventh damage state are the same at every storey level, because of the assumption that the collapse of any storey will imply the collapse of the entire building. While in the sixth damage state the

TMD still achieves a substantial cost reduction for both mass ratios (83% for μ = 5% and 81% for μ = 10%), no cost reduction is obtained within the seventh damage state, where the control proves in fact detrimental, leading to costs which are increased with respect to the uncontrolled ones to, respectively, 108% for μ = 5% and 114% for μ = 10%.

Figure 5 Lifetime costs for the uncontrolled and controlled cases, distributed among storey levels and damage states, (a) uncontrolled – μ = 0% (b) controlled – μ = 5% (c) controlled – μ = 10% (see online version for colours)

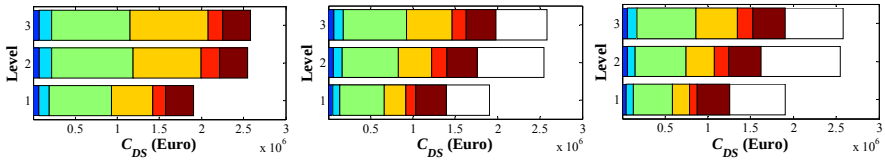

(a) (b) (c)

Note: Legend for the damage states, from left to right: 1 (dark blue, not shown); 2 (blue); 3 (azure); 4 (green); 5 (orange); 6 (red); 7 (brown).

Figure 6 is the analogue of Figure 5, except that the cost is now decomposed in cost categories instead of damage states. For the uncontrolled case, the category which contributes the most is damage repair (47%), followed by income (21%), loss of content (16%) and fatalities (14%). For the two controlled cases, the order gets slightly modified, with the most significant category still being damage repair (about 44%), now followed by fatalities (about 21%), income (about 19%) and loss of content (about 15%). In all cases, the remaining three categories, i.e., rental, minor and serious injuries, contribute all together to less than 2%. It deserves mentioning that the cost of fatalities, which as a percentage of the overall cost appears larger in the controlled cases than in the uncontrolled case (about 21% versus 14%), is however nearly the same for both the uncontrolled and the controlled cases in absolute terms, namely reducing to 99% of the uncontrolled value for μ = 5% and increasing to 103% for μ = 10%. This circumstance makes the obtained global cost predictions be only moderately affected by the large uncertainty inherent in the value attributed to the cost of human lives.

Figure 6 Lifetime costs for the uncontrolled and controlled cases, distributed among storey levels and cost categories, (a) uncontrolled – μ = 0% (b) controlled – μ = 5% (c) controlled – μ = 10% (see online version for colours)

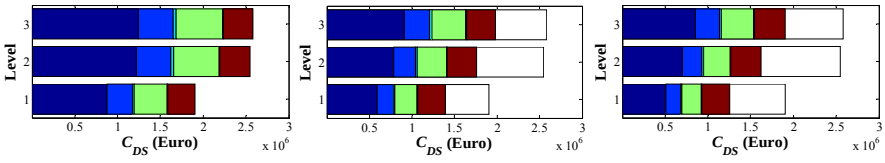

(a) (b) (c)

Note: Legend for the cost categories, from left to right: C^i_{dam} (dark blue); C^i_{con} (blue); C^i_{ren} (azure); C^i_{inc} (green); $C^i_{inj,m}$ (orange); C^i_{inj} (red); C^i_{fat} (brown)

Summing along the building height, the total damage cost (C_{DS}) for the uncontrolled structure turns out to be $7.03 \cdot 10^6$ € (corresponding to 1168 €/m^2). For the 5% and 10% controlled cases, that cost drops to, respectively, $5.13 \cdot 10^6$ € (852 €/m^2) and $4.78 \cdot 10^6$€ (794 €/m^2), resulting in cost reduction ratios equal to, respectively, 73% and 68%. The lifetime cost saved by the TMD is therefore $1.90 \cdot 10^6$ € for μ = 5% and $2.25 \cdot 10^6$ € for μ = 10%; remarkably, doubling the TMD mass increases savings by only a factor of 1.18. Although a detailed cost-benefit analysis exceeds the scope of this paper, preliminary estimates indicate that these savings are much larger than the cost necessary for designing, building and maintaining the TMD system, particularly if the 5% mass ratio is adopted. Repeating the LCC analysis by using a mechanically linear model instead of the bilinear one would reveal a considerably improved TMD effectiveness. For, respectively, the 5% and 10% mass ratios, cost reduction ratios would be 61% and 52% for the linear model instead of the 73% and 68% values obtained above for the non-linear structure.

4 Conclusions

In this paper a methodology for evaluating the cost-effectiveness of passive TMDs on non-linear MRF building structures located in high seismicity regions is introduced and exemplified on the three-storey SAC steel benchmark building. The method is a slight variant of previous LCC multi-hazard approaches, relying on MSDA to compute the occurrence probability of multiple damage states expressed in terms of peak inter-storey drift ratios. According to this variant, a new formula is proposed for relating exceedance frequencies and drift ratios [equation (9)], and damage costs are computed independently at all storey levels. By estimating, for the original uncontrolled building as well as for two possible TMD installations (respectively μ = 5% and 10%), the expected cost of future earthquake damages and losses, the illustrative case study infers the economic advantage of implementing the control action.

Results confirm that TMDs on non-linear structures perform acceptably well under moderate earthquake loading, when the structure remains linear or weakly non-linear, but may lose effectiveness and even prove detrimental under severe ground shaking, when strong non-linearities occur. Traditional performance criteria, computed under various increasing hazard levels, are inadequate to uniquely and concisely assess the control convenience, because unable to weigh, on a physically sound, economic basis, the relative significance of the various hazard scenarios.

By determining, for each damage state, its probability of occurrence and its expected lifetime cost, the LCC approach can provide, instead, a rational and comprehensive measure of TMD performance, directly expressed in monetary units and then immediately useable by decision-makers for asset management purposes. By adopting this LCC perspective, for the case study under examination, a TMD having a mass ratio of, respectively, 5% and 10% is shown to reduce the building lifetime cost to, respectively, 73% and 68% of its uncontrolled value. According to gross cost estimations, cost savings achieved through TMD installation can largely compensate the cost necessary for designing, building and maintaining the TMD system, particularly if the 5% mass ratio is adopted. By decomposing the overall LCC into partial cost components, large reductions are observed in costs associated with intermediate damage states (‘4 – moderate’ and ‘5 – heavy’) and satisfactory reductions are obtained within the sixth

damage state (‘6 – major’) too. No cost reductions are instead observed within the most severe damage state (‘7 – destroyed’), corresponding to building collapse. On the contrary, as a consequence of TMD inefficacy in the event of large building inelastic excursions, collapse-related costs increase to 108% for μ = 5% and to 114% for μ = 10%, whereas the absolute cost of human fatalities appears nearly unaffected by the presence of the absorber. Such counter-productive effect of TMDs in the event of a collapse indicates that, contrary to what is observed on linear structures, for inelastic structures the advantage of a large mass ratio may be confined to small-to-moderate hazard levels, so that the marginal benefit of further increasing the absorber mass ratio (beyond, e.g., the 5% value adopted here) may result of no practical interest.

In conclusion, the proposed LCC estimation approach proves a powerful criterion for evaluating the seismic cost-effectiveness of TMDs on inelastic structures, and the presented case study shows that, for typical low-rise steel MRF buildings located in high seismic areas, despite the poor control performance exhibited against the most severe hazard scenarios, nonetheless TMDs may be of significant practical advantage in reducing the economic consequences of seismic damages and losses. The application of such a criterion to the optimal design of TMDs on inelastic structures is currently under way and will be the object of future works.

References

FEMA-273 (1997) *NEHRP Guidelines for Seismic Rehabilitation of Buildings*, Federal Emergency Management Agency, Washington, DC.

Fragiadakis, M. and Lagaros, N.D. (2011) ‘An overview to structural seismic design optimisation frameworks’, *Computers and Structures*, Vol. 89, Nos. 11–12, pp.1155–1165.

Ghobarah, A. (2004) ‘On drift limits associated with different damage levels’, *Proceedings of the International Workshop on Performance-based Seismic Design – Concepts and Implementation*, Bled, Slovenia, pp.321–332.

Ghobarah, A., Abou-Elfath, H. and Biddah, A. (1999) ‘Response-based damage assessment of structures’, *Earthquake Engineering and Structural Dynamics*, Vol. 28, No. 1, pp.79–104.

Gupta, A. and Krawinkler, H. (1999) *Seismic Demands for Performance Evaluation of Steel Moment Resisting Frame Structures*, Report No. 132, June, The John A. Blume Earthquake Engineering Center, Stanford University, Stanford, CA.

Hahm, D., Ok, S-Y., Park, W., Koh, H-M. and Park, K-S. (2013) ‘Cost-effectiveness evaluation of an MR damper system based on a life-cycle cost concept’, *KSCE Journal of Civil Engineering*, Vol. 17, No. 1, pp.145–154.

Hoang, N., Fujino, Y. and Warnitchai, P. (2008) ‘Optimal tuned mass damper for seismic applications and practical design formulas’, *Engineering Structures*, Vol. 30, No. 3, pp.707–715.

Kappos, A.J. and Dimitrakopoulos, E.G. (2008) ‘Feasibility of pre-earthquake strengthening of buildings based on cost-benefit and life-cycle cost analysis, with the aid of fragility curves’, *Natural Hazards*, Vol. 45, No. 1, pp.33–54.

Kaynia, A.M., Veneziano, D. and Biggs, J.M. (1981) ‘Seismic effectiveness of tuned mass dampers’, *Journal of Structural Engineering*, Vol. 107, No. 8, pp.1465–1484.

Lagaros, N.D., Fotis, A.D. and Krikos, S.A. (2006) ‘Assessment of seismic design procedures based on the total cost’, *Earthquake Engineering and Structural Dynamics*, Vol. 35, No. 11, pp.1381–1401.

Lukkunaprasit, P. and Wanitkorkul, A. (2001) 'Inelastic buildings with tuned mass dampers under moderate ground motions from distant earthquakes', *Earthquake Engineering and Structural Dynamics*, Vol. 30, No. 4, pp.537–551.

Matta, E. (2011) 'Performance of tuned mass dampers against near-field earthquakes', *Structural Engineering and Mechanics, an International Journal*, Vol. 39, No. 5, pp.621–642.

Matta, E., De Stefano, A. and Spencer Jr., B.F. (2009) 'A new passive rolling-pendulum vibration absorber using a non-axial-symmetrical guide to achieve bidirectional tuning', *Earthquake Engineering and Structural Dynamics*, Vol. 38, No. 15, pp.1729–1750.

Mitropoulou, C.C., Lagaros, N.D. and Papadrakakis, M. (2011) 'Life-cycle cost assessment of optimally designed reinforced concrete buildings under seismic actions', *Reliability Engineering and System Safety*, Vol. 96, No. 10, pp.1311–1331.

Ohtori, Y., Christenson, R.E., Spencer Jr., B.F. and Dyke, S.J. (2004) 'Benchmark control problems for seismically excited nonlinear buildings', *Journal of Engineering Mechanics*, Vol. 130, No. 4, pp.366–385.

Pinkaew, T., Lukkunaprasit, P. and Chatupote, P. (2003) 'Seismic effectiveness of tuned mass dampers for damage reduction of structures', *Engineering Structures*, Vol. 25, No. 1, pp.39–46.

Sladek, J.R. and Klingner, R.E. (1983) 'Effect of tuned mass dampers on seismic response', *Journal of Structural Engineering*, Vol. 109, No. 8, pp.2004–2009.

Somerville, P., Smith, N., Punyamurthula, S. and Sun, J. (1997) *Development of Ground Motion Time Histories for Phase 2 of the FEMA/SAC Steel Project*, SAC Background Document, Report No.SAC/BD-97/04.

Soto-Brito, R. and Ruiz, S.E. (1999) 'Influence of ground motion intensity on the effectiveness of tuned mass dampers', *Earthquake Engineering and Structural Dynamics*, Vol. 28, No. 11, pp.1255–1271.

Taflanidis, A.A. and Beck, J.L. (2009) 'Life-cycle cost optimal design of passive dissipative devices', *Structural Safety*, Vol. 31, No. 6, pp.508–522.

Warburton, G.B. (1982) 'Optimum absorber parameters for various combinations of response and excitation parameters', *Earthquake Engineering and Structural Dynamics*, Vol. 10, No. 3, pp.381–401.

Wen, Y.K. and Kang, Y.J. (2001) 'Minimum building life-cycle cost design criteria II: applications', *Journal of Structural Engineering*, Vol. 127, No. 3, pp.338–346.

Wong, K.K.F. (2008) 'Seismic energy dissipation of inelastic structures with tuned mass dampers', *Journal of Engineering Mechanics*, Vol. 134, No. 2, pp.163–172.

Wong, K.K.F. and Harris, J.L. (2012) 'Seismic damage and fragility analysis of structures with tuned mass dampers based on plastic energy', *The Structural Design of Tall and Special Building*s, Vol. 21, No. 4, pp.296–310.

Zhang, Z. and Balendra, T. (2013) 'Passive control of bilinear hysteretic structures by tuned mass damper for narrow band seismic motions', *Engineering Structures*, Vol. 54, pp.103–111.